LAWRENCE
LIVERMORE
NATIONAL
LABORATORY

LLNL-JRNL-564236

Controlling the Actuation Rate of Low Density Shape Memory Polymer Foams in Water

P. Singhal, T. Boyle, S. Infanger, S. Letts, W. Small, D. J. Maitland, T. S. Wilson

July 12, 2012

Macromolecular Chemistry and Physics

Disclaimer

((please add journal code and manuscript number, e.g., DOI: 10.1002/macp.201100001))
Article type: Full Paper

Controlling the Actuation Rate of Low Density Shape Memory Polymer Foams in Water

Pooja Singhal, Anthony Boyle, Stephen Infanger, Steve Letts, Ward Small, Ya-Jen Yu, Duncan J. Maitland*, Thomas S. Wilson*

Pooja Singhal, Anthony Boyle, Stephen Infanger, Dr. Duncan J. Maitland
Department of Biomedical Engineering, 5045 Emerging Technologies Building
3120 TAMU, College Station, TX-77843, USA
E-mail: wilson97@llnl.gov, duncanjmaitland@tamu.edu; Fax: 979-845-4450

Pooja Singhal, Dr. Steve Letts, Dr. Ward Small, Dr. Thomas S. Wilson
7000 East Avenue, Physical and Life Sciences Directorate, Lawrence Livermore National Laboratory, Livermore CA-94550, USA

Shape memory polymers (SMPs) have been shown to actuate below their dry glass transition temperatures in the presence of moisture due to plasticization. This behavior has been proposed as a self-actuating mechanism of SMPs in water/physiological media. However, control over the SMP actuation rate, a critical factor for *in vivo* transcatheter device delivery applications, has not been previously reported. Here we describe a series of polyurethane SMPs with systematically varied hydrophobicity, which permits control of the time for their complete shape recovery in water from under 2 minutes to more than 24 hours. This control over the SMP actuation rate can potentially provide significant improvement in their delivery under conditions which may expose them to high moisture environments prior to actuation.

Introduction

Shape memory polymers (SMPs) are an emerging class of materials which can remember two or more shapes, and can be actuated to go from one shape to another via an external stimulus such

as heat or light. Several comprehensive reviews discussing the properties and behavior of these *"smart"* materials have been published.[1-5] Processing these SMPs into low density foams is an active area of research. Hayashi et al. proposed a series of polyurethane SMP foams[6], which have subsequently been studied extensively.[7-10] Other polyurethane and epoxy based SMP foam compositions have been reported and characterized in the literature more recently.[11-13] These SMP foams exhibit unique properties such as low density, high volume expansion on actuation, and high thermal/electrical insulation, which allow for a myriad of potential applications in the aerospace, clothing, sporting gear, and biomedical industries.[14] Among a multitude of potential biomedical applications (e.g. tissue regeneration scaffolds and embolic foams), [15-19] our group is particularly interested in using SMP foams for embolic devices for the treatment of aneurysms.

The ability of low density SMP foams to stay in a miniaturized compressed form, until actuated to their primary large volume shape, is especially desirable for minimally invasive endovascular applications.[18,19] However, despite their unique properties, the practical use of SMP foams in such applications is quite in its infancy. One of the key issues seen with these materials is the loss of their ability to *"actuate on demand"*. This may happen by: a) loss of the material's tendency to actuate following storage in a secondary shape over long periods of time or at relatively high temperatures (referred to as secondary-shape forming [9] and addressed in an earlier publication [11]) and/or b) premature actuation, such as on exposure to moisture, a plasticizing agent, which depresses the actuation temperature of the foams.[20,21] The phenomenon of actuation of SMP foams in the presence of moisture, and thereby the loss of their *"on demand"* actuation, is investigated here.

The effect of moisture on the actuation of SMPs has been reported previously as an alternate actuation mechanism.[22-24] Huang et al. described several "water-actuated" neat/non-porous and porous SMP devices based on the MM 3520, MM 3550, and MM 5510 materials from Mitsubishi Heavy Industries.[22,23] Jung et al. reported polyurethane SMP films based on poly(ethylene glycol) (PEG), polyhedral oligomeric silsesquioxane (POSS) and 1,4-phenyldiisocyanate.[24] These films had a hydrophilic soft segment comprising PEG and a hydrophobic hard segment containing POSS. They demonstrated water-responsive shape recovery of more than 70% for all samples at 30 ºC, depending on the POSS content of the films.[24] Yang et al. investigated the mechanism of actuation of SMPs with water on MM 3520 films, and found that it is a combined effect of the weakening of the hydrogen bonding between N–H and C=O groups and plasticization caused by the small water molecules.[25] SMP foams from our group [11] were tested for the effect of moisture by Yu et al., and again the above mechanisms were found to be at work in quickly depressing the glass transition temperature (*Tg*) of the foam and causing its rapid actuation on exposure to water.[21]

The passive self-actuation of a thermally responsive SMP device in water or physiological media at body temperature may be a useful feature for a simpler device deployment mechanism without a heating capability. However, if the passive actuation occurs too quickly or in an uncontrollable manner, it can cause problems. For example, usage of SMP foams for minimally invasive treatment of aneurysms requires transcatheter delivery of the device in its compressed cylindrical shape. Once it reaches the target site, it would be actuated to its primary spherical shape to fill the aneurysm and, eventually, resist any blood flow inside it. Since the compressed device may be exposed to moisture/physiological fluid while inside the catheter, premature expansion of a

moisture-sensitive device may occur during the delivery itself. This can drastically increase the friction within the catheter and potentially inhibit delivery of the device. With low density foams, this issue becomes even more important due to the increased surface area available for the uptake of water/moisture. Hence, it is desirable to be able to control the rate of actuation of the foam based SMP devices in the presence of moisture.

One possible solution to this problem would be to vary the hydrophobicity of the SMP, thereby controlling the extent of the depression in actuation temperature due to exposure to water. To test this hypothesis, we synthesized and characterized a novel series of low density SMP foams with increasing diisocyanate monomer hydrophobicity. Such materials should exhibit a controlled reduction in the rate of their self-actuation in water, facilitating transcatheter delivery of the device. Here we report the process of synthesis of these materials, their key physical properties, and their actuation behavior. Also, an analysis of the actuation mechanism is presented, and various challenges and potential solutions to the transcatheter delivery of SMP foam devices are discussed.

Materials and Methods

Synthesis

N,N,N',N'-Tetrakis (2-hydroxypropyl) ethylenediamine (HPED, 99%, Sigma Aldrich Inc.), 2,2',2"-Nitrilotriethanol (TEA, 98%, Alfa Aesar Inc.), 1,6-Diisocyanatohexane (HDI, TCI America Inc.), 1,6-Diisocyanato-Trimethylhexane, 2,2,4- and 2,4,4- mixture (TMHDI, TCI America Inc.), and DI water (Millipore water purifier system, Millipore Inc., >17 MΩ·cm purity), were used as received. Foams were synthesized in a three step method reported

previously [11], using the amounts indicated in **Table 1**, and were allowed to cure for at least a week before testing. The notations 100TM, 80TM, 60TM, 40TM, 20TM and 0TM denote TMHDI constituting 100, 80, 60, 40, 20 and 0 wt.% of isocyanate respectively, with the remaining wt.% of isocyanate coming from HDI, as indicated in Table 1.

Neat polymers of corresponding compositions, excluding the physical and chemical blowing agents and other foaming additives (surfactants and catalysts), were synthesized according to **Table 2** for contact angle measurements. Calculated amounts of monomers were mixed together and cast in polystyrene dishes. The curing profile involved an initial cure at room temperature for 2 hours followed by ramping up to 120 ºC at 20 ºC·hr^{-1}. Thereafter, the temperature was maintained at 120 ºC for 2 hours, and finally the heat was turned off and samples were allowed to cool down to room temperature. An inert nitrogen atmosphere was maintained throughout the curing process.

Post-processing of foams

Post-processing of foams is often required since the as-blown foams typically retain residual membranes post-synthesis. In order to make foams completely open cell or reticulated, as desired for the proposed application, secondary physical processes such as hydrolysis, oxidation, heat or mechanical treatment are normally employed.[26] Caustic hydrolysis of polyurethanes, also referred to as “quenching”, is a standard process of reticulation of traditional polyurethane foams in industry.[27] Another well accepted method of reticulating polyurethane foams is “zapping”, which involves controlled burning of the membranes via saturation with flammable gases.[27] Several patents have been filed in this area of study.[28-33]

In this work an acid-based etching was performed on the foams prior to testing of their actuation and actuation related properties. Although this etching process was not optimized for complete membrane removal in the foams, it was included to account for the possibility that more hydrophilic surfaces may be created from these post-processing etching methods.[34] Since increased surface hydrophilicity may alter the moisture sensitivity of the material relative to un-etched foams, the device actuation results with inclusion of the etching process are potentially more relevant to an actual device. For performing the cleaning and etching processes, blocks of foams were etched in hydrochloric acid (0.1 N, BDH Chemicals) for 2 hours. Thereafter they were cleaned with two 15 minute treatments each of 80-20 vol.% DI water-Contrad solution and DI water, respectively. All steps were performed under sonication. The foams were finally dried overnight under vacuum at 50 ºC before testing.

Physical properties

Density and cell structure

Core densities of three foam samples of each composition were measured from the representative top and middle sections as per the ASTM standard D-3574. For cell structure characterization, thin slices of foam were cut from a representative top section of the blown foam, and images were captured in the brightfield mode on a Leica MZ8 microscope (Leica Microsystems Inc.) using RSImage Software (Roper Scientific Inc.).

Differential Scanning Calorimetry (DSC)

Glass transition temperature (*Tg*) was measured using a Q-200 DSC (TA Instruments Inc.). A 3-5 mg sample was loaded in a vented aluminum pan at room temperature, cooled to -40 ºC and then run through a heat - cool - heat cycle from -40 to 120 ºC at 10 ºC·min^{-1}. The half height of the transition during second heat was taken as an estimate of the *Tg*.

Dynamic Mechanical Analysis (DMA)

For characterizing the mechanical properties of the foams as a function of temperature, a dynamic temperature ramp test was performed on an ARES-LS2 Rheometer (TA Instruments Inc.) according to a previously described method.[11] A torsion rectangle test fixture was used on samples cut to approximately 45 mm long, 12 mm wide, and 6 mm thick with a gap distance of 25 mm. The samples were prepared by embedding both ends in a polyurethane neat polymer to prevent damage and slippage of the foam sample in the metal grips. Dynamic temperature ramp tests were then run for each formulation in triplicate, at a frequency of 1 Hz and constant heating rate of 1 ºC·min^{-1} from 25 ºC to 150 ºC. An initial shear strain of 0.2% was used. However, as the temperature increased, the strain was adjusted by the control software to maintain a torque range of 0.5 to 5 g·cm, allowing a maximum strain of 10% (still within the linear viscoelastic region) at high temperatures. Data points were collected every 5 seconds. Dynamic shear storage modulus (*G'*), dynamic shear loss modulus (*G"*), and their ratio *tan* δ (=*G"*/*G'*) were recorded using the Orchestrator™ software (TA Instruments Inc.). T_{onset} was recorded as the temperature at which the baseline and the leading edge of the peak in *tan* δ intersect, $T_{\delta s}$ (another measure of *Tg*) was recorded as the temperature at which the *tan* δ curve was at its peak value, and ΔT (breadth of transition) was recorded as twice the difference between $T_{\delta s}$ and T_{onset}, according to Yackaki et al.[35]

Fourier Transform Infrared Spectroscopy (FTIR)

An FTIR spectrum of the foam was collected using a Spectrum 2000 FTIR (Perkin Elmer Inc.). The sample chamber was purged with nitrogen gas for 5 minutes and a background spectrum was captured. Thereafter, thin slices cut from foam blocks (~2-4 mm in thickness) were placed on a 2 cm^{-1} JStop holder (0.88 cm aperture). The chamber was again purged for 5 minutes after placing the sample, and an FTIR spectrum was collected in the transmission mode at a resolution of 4 cm^{-1}. The test was performed in duplicate to ascertain reproducibility of the spectra. A total of 50 scans were taken for each sample and the background spectrum was subtracted using the Spectrum software (Perkin Elmer Inc.).

Characterization of foam actuation and actuation-related properties

Contact angle

Contact angle measurements were made on neat/unfoamed polymers corresponding to the foam compositions (Table 2) using a DSA100 (Kruss Inc.). DI water drops of 4-5 ml volume were placed on the sample surface. The drop was allowed to come to an equilibrium shape for 30 seconds and the resulting contact angle was measured using the drop shape analysis software (Kruss Inc). An average value over 10 measurements was calculated for an estimate of the contact angle of the polymer surface.

Equilibrium water uptake

Cylindrical foam samples were cut from a 2.5 cm thick foam block using an 8 mm diameter biopsy punch and dried under vacuum at 50 ºC overnight. The dry sample weight (W_{dry}) was

measured on an Ohaus Analytical Plus scale (Central Carolina Scale Inc.). The samples were then soaked in ~1000 times weight excess of water for 24 hours. To measure the equilibrium water absorption, the samples were first taken out from water media and the excess (adsorbed) water on the samples was removed in two steps: a) repeated pressing (by hand) between sheets of laboratory grade kimwipes (Kimberly-Clark Inc.), until no wet spots could be seen, and then b) pressing between kimwipes to 1 metric ton pressure for 2 minutes in a #3925 Hydraulic press (Carver Laboratory Equipments). The samples were placed on the weighing balance immediately thereafter and their equilibrium weight (W_{wet}) was recorded. The absorbed water (wt.%) in the foam samples was calculated as $(W_{wet} - W_{dry}) * 100/W_{dry}$. Five samples were tested for each foam composition.

Depression in *Tg* with exposure to water

Cylindrical samples of foam were cut from a 2.5 cm thick block using an 8 mm diameter biopsy punch and submerged in a water bath at 37 ºC for 5, 15, 30, 60, or 120 minutes. After the specified time of submersion, the samples were taken out and excess water was removed in two steps using kimwipes and a hydraulic press as described above. A DSC scan was then run from −40 to 80 ºC at 10 ºC·min^{-1} on a 4-8 mg foam sample in a vented aluminum pan, using a Q-200 DSC (TA Instruments Inc.). The *Tg* of the sample was estimated from the half height of the thermal transition during the first heating scan. Five samples of each composition were tested at each time point.

Rate of expansion of foam in water at 37 ºC

Cylindrical foam samples approximately 1 cm in length were cut using a 6 mm diameter biopsy punch and threaded over straight 0.09 mm diameter Nitinol wires (Nitinol Devices & Components, Inc.). An initial measurement of the diameter of the punched samples was taken using a digital micrometer. Each sample was then radially compressed as small as possible, at 97 ºC, using an SC150-42 Stent Crimper (Machine Solutions Inc.). The compressed shape was fixed by allowing the sample to cool down to room temperature in the compressed state. The samples were allowed to rest in this secondary compressed shape for 24 hours in a nitrogen purged environment before testing. After the resting period, the compressed diameter was measured using a digital micrometer. The nitinol wires holding the compressed foam samples were then strung across a heavy fixture such that the foam never touched the fixture, and the assembly was submerged in a water bath heated to 37.0 ± 0.5 ºC. A scale was submerged alongside the samples. Images of the foam samples were taken at 1 to 5 minute intervals over a period of 1 hour, as the foams expanded in the water bath. For the measurement of the diameter of the foam at any given time, the maximum diameter along the length of the sample was measured from the captured images using ImageJ software. Five samples of each composition were tested. Results were normalized by the measured initial (uncompressed) diameter.

Theoretical solubility parameter analysis

Hoy's solubility parameters were calculated to estimate the relative swelling of the foams in the water media.[36] The calculations were done based on the 4 types of network units generated from the reaction of isocyanate with HPED, TEA, water, and the excess isocyanate. While the excess isocyanate groups can undergo several secondary reactions such as allophanate or biuret formation, for simplicity they were assumed to be converted to primary amines from reaction

with ambient moisture. Group contributions of each of these network units, HPED, TEA, water, and excess isocyanate **(Figure 1)** were calculated as per Van Krevelen et al.[36] The net solubility parameter components δ_t, δ_p and δ_h representing total, polar and hydrogen bonding components of the polymer cohesive energy density, were then determined by adding the respective contributions of the network units on a volume fraction (ϑ) basis (Equation 1). The dispersion force component of the total solubility parameter was calculated using Equation 2.

$$\delta = \delta_{HPED} * \vartheta_{HPED} + \delta_{TEA} * \vartheta_{TEA} + \delta_{water} * \vartheta_{water} + \delta_{excess} * \vartheta_{excess} \text{ ,here } \delta = \delta_t \text{ or } \delta_p \text{ or } \delta_h \quad (1)$$

$$\delta_d = \sqrt{(\delta_t^2 - \delta_p^2 - \delta_h^2)} \quad (2)$$

Results

Physical properties

Density and cell structure

Density results of all foam compositions are reported in **Table 3**. Sufficiently low density foams were seen for all foams with values ranging from 0.013 to 0.027 g·cm^{-3}. These values suggest an average porosity $[= (\rho_{neat} - \rho_{porous})/\rho_{neat}]$ of ~98% and a high average theoretical volume expansibility $(= \rho_{neat}/\rho_{porous})$ of ~ 60 times; here average $\rho_{neat} \sim 1.1\ g \cdot cm^{-3}$ is the neat polymer density and ρ_{porous} is the foam density. The small standard deviation of 0.001 - 0.006 g·cm^{-3} (Table 3) in the density measurements indicates a fairly uniform structure of the foams.

Optical microscopy was used to determine cell structure, with typical structures shown in **Figure 2.** Observations include uniform closed or mixed closed to open cell structure for a given

composition, with thin residual membranes between struts as previously reported for similar materials.[11] At the same time cell sizes varied for the different compositions. A significant factor contributing to the size variation is believed to be the variation in the foaming solution viscosity (~2 Pa·s to 60 Pa·s), which was not a controlled variable across different compositions. It has been observed that the cell sizes of the foams can be controlled by controlling the viscosity of the foaming solution; the sizes are generally seen to decrease with increase in the foaming solution viscosity.

It is important to note here that the primary design objectives for the proposed application (low density and uniform cell structure) as described in Singhal et al.[11] were successfully met for all compositions. Hence, properties specific to the embolic biomedical applications of these materials, such as high crimping efficiency of the device and a large volume expansion on actuation, may be realized. Also, they have a highly crosslinked network architecture, which is expected to provide optimal shape memory properties as described by Singhal et al. [11]

Differential Scanning Calorimetry (DSC)

DSC results of the foams are shown in Table 3 and **Figure 3**. The foams show a single *Tg* with values varying within a narrow range of 63-75 ºC. Lack of any crystallization or melting region in the DSC thermogram confirms the amorphous nature of the polymer network. An increase in the TMHDI content was seen to increase the effective *Tg* of the foams. This is expected as the methyl groups of TMHDI can increase the energy required by the molecule to rotate about the backbone bonds.

Dynamic Mechanical Analysis (DMA)

DMA results of the foams are shown in Table 3 and **Figure 4**. A variation in the glassy modulus (G'_{glassy}) is recorded from 311 kPa to 90 kPa across different compositions. To explain this relatively large range, variation in the densities of these compositions were accounted for in the G'_{glassy} estimations. The reference of 0TM was used and the value of G'_{glassy} at 0.018 g·cm^{-3} was extrapolated using $G_1 = G_2(\rho_1/\rho_2)^2$ as per Gibson and Ashby et al.[37], where G is the modulus, ρ is the material density, and subscripts 1 and 2 denote corrected and measured values, respectively. Average glassy moduli of ~70, 101, 161, 197, and 179 kPa were thus calculated for 20TM, 40TM, 60TM, 80TM, and 100TM foams, respectively. While the values of other compositions are similar when extrapolated to the same density, 20TM and 40TM foams have relatively lower moduli (70-101 kPa). This may be due to larger cell sizes of these foams as seen in Figure 2. Surface effects have been shown to become more prominent as the dimensions of the tested sample approach those of the cell size, and a reduction in foam modulus and strength is often noticed in such cases.[38,39]

The DMA measured *Tg* of all the materials is within ~16 ºC, leading to a significant overlap in the storage modulus vs. temperature curves (Figure 4). The onset of transition from the glassy to the rubbery state is approximately 55±3 ºC, and *Tg* (estimated as the temperature at the peak value of the *tan* δ curve) is 72±7 ºC across all compositions (Table 3). A small but positive increase in the *Tg* with increase in the TMHDI content is seen. This follows the trend observed in the DSC measurements (Figure 3). Also, a single thermal transition from the glassy to the rubbery state, with a transition range of ~35±6 ºC was recorded for all compositions. The

presence of a single thermal transition with a constant rubbery modulus confirms an amorphous and crosslinked polymer network structure of the foams.

Fourier Transform Infrared Spectroscopy (FTIR)

The FTIR spectra of the foams of different compositions are shown in Figure 5. The spectra of the compositions are qualitatively similar, and the typical features of the spectra reported earlier for related compositions [11] are evident for all compositions. These include the hydrogen bonded urethane peak at ~1695 cm^{-1} and a urea shoulder at ~1653 cm^{-1}. The position of these peaks, however, is shifted (~3-6 cm^{-1} higher) compared to previously reported foams.[11] This may be related to the difference in the physical condition of the tested samples.[40] The compression of the foams to a flat sheet for performing Attenuated Total Reflectance (ATR) -FTIR done in the previous study [11] may have enhanced hydrogen bonding of urethane/urea groups leading to a shift of urethane and urea absorption to slightly lower values.

On the other hand, the effect of TMHDI can be readily observed across the different compositions. The differences in the C-H vibrations due to the inclusion of methyl side groups of TMHDI can be seen in the 2800-3000 cm^{-1}, 1430-1490 cm^{-1} and 1350-1400 cm^{-1} wavenumber ranges. The peaks at 2958 cm^{-1} and 2871 cm^{-1} in the 100TM foam correspond to asymmetrical and symmetrical C-H stretching vibrations of the -CH_3 groups, respectively.[41] The peaks at 1464 cm^{-1} and 1370 cm^{-1} in the 100TM foam correspond to the asymmetrical and symmetrical C-H deformation vibrations of the -CH_3 groups, respectively [41]. These peaks are seen to increase in intensity due to an increase in the C-H vibration as the amount of TMHDI is increased.

Characterization of foam actuation and actuation-related properties

Contact angle

The contact angle was measured on neat/unfoamed polymer samples as these measurements on foam samples were difficult, and subject to high variability due to the porous nature of the foam surface. The measurement results of the corresponding compositions are shown in **Table 4,** and **Figure 6** illustrates the change in contact angle as we progress from the 0TM to the 100TM composition. A decrease in the contact angle from 78 to 62 degrees is seen as the TMHDI content is decreased in the composition. This result supports the hypothesis that the introduction of methyl groups in the polymer network via use of TMHDI increases the hydrophobicity of the material. Although the absolute values of contact angle for the corresponding foam formulations can be different from those obtained from the neat samples due to the presence of urea groups from the use of water as a chemical blowing agent in the foams, they are expected to follow a similar trend with the variation in the foam composition.

Equilibrium water uptake

Equilibrium water absorption values are reported in Table 4. Water uptake decreases from ~8% to ~2% as the TMHDI content is increased in the foam composition. This result is in agreement with the contact angle results, and is a direct measure of the increase in hydrophobicity of the foams with increasing TMHDI content.

Depression in *Tg* with exposure to water

The results of depression in the foam *Tg* on its exposure to water are shown in Table 4 and **Figure 7**. All foam compositions reach their equilibrium plasticized *Tg* value within 5 minutes of exposure to water. Kinetically, the depression in *Tg* is fast enough that it may be considered independent of the TMHDI composition within the tested time scale. The extent of depression of *Tg*, however, progressively decreases as the TMHDI content is increased, with the equilibrium *Tg* value going from ~12 ºC for the 0TM foams to ~40 ºC for the 100TM foams. Consequently, the extent of plasticization due to moisture is found to be lower (higher equilibrium *Tg* ~40 ºC) for the most hydrophobic polymer composition.

Rate of expansion of foam in water at 37 ºC

Results of the rate of expansion of foam samples in water are shown in Table 4 and **Figures 8 and 9.** The rate of actuation decreases with increase in the amount of TMHDI in the foam formulation. The 0TM foam samples show no delay in actuation and achieve complete actuation within 2 minutes of exposure to water. Conversely, 100TM foam samples maintain their secondary compressed shape for ~10 minutes under water, and do not recover completely to their primary shape even after 1 hour. The error bars in Figure 9 are relatively large due to the fact that the maximum diameter of the expanding foams was used to generate the plot. As is evident in Figure 8, even though the average trend of actuation is the same within a given composition, the maximum diameter is not uniform across the entire length of the sample and varies across different samples of the same composition.

The foam actuation rate depends on the depressed *Tg* in the water and the temperature of the water. Since the depressed *Tg* of the 100TM foam is ~40 ºC (i.e., slightly above the water

temperature), it does not actuate as readily as the 0TM foam whose depressed *Tg* of ~12 ºC is well below the water temperature (37 ºC). It should be noted here that although these tests are conducted in water, the foams are expected to have a similar trend of actuation behavior in physiological media due to its high water content.

Theoretical solubility parameter analysis

Hoy's solubility parameters calculated for different polymer compositions are reported in **Table 5.** The objective of doing these calculations was to develop an understanding of the changes in the solvent (water) – polymer interactions with the variation in the polymer formulation. It is well known that the difference between the solubility parameter (δ_t) value of a crosslinked polymer and that of the solvent is directly related to the degree of polymer swelling in that solvent.[36] The calculated net δ_t of 0TM and 100TM compositions are 23.0 and 21.3 $J^{1/2}\cdot cm^{-3/2}$ respectively, resulting in a higher difference in the polymer and water δ_t values for the 100TM composition ($\delta_{t\ water}$ = 48 $J^{1/2}\cdot cm^{-3/2}$). This suggests that the 0TM foams would undergo a higher equilibrium swelling in water compared to the 100TM foams, due to their relatively favorable chemical environment in water. The higher extent of equilibrium swelling is expected to influence the depression in *Tg*, and therefore the rate of actuation of the foam devices in water.

To better understand the foam actuation mechanisms, we now discuss the effect of the polymer chemical structure on its interaction with water. In previous studies it has been found that the water molecules weaken the hydrogen bonding between N–H and C=O groups and plasticize the polymer network, causing a depression in the *Tg* of the polyurethane SMP materials in high humidity/water environments.[20,21,25] Water molecules have a small size and a high hydrogen

bonding potential. Hence, when exposed to a polyurethane SMP, they can disrupt the hydrogen bonds between N–H and C=O groups of the urethane linkages of adjacent chains, and can then be inserted between these groups via mutual hydrogen bonding. Since hydrogen bonding is largely dynamic in nature, insertion of water molecules between adjacent chains essentially works as a lubricant, thereby increasing the mobility of the chains, i.e. plasticizing the polymer.[42] By this analogy, the change in the degree of depression of *Tg* seen for the series of compositions here should be a function of the extent of interaction of water molecules with the urethane hydrogen bonding in the polymer. Indeed, as demonstrated by the water absorption studies and the theoretical determination of solubility parameters, the amount of equilibrium water absorbed depends on the chemical environment of the polymer. Due to higher differences in the cohesive energy densities, it is relatively energetically unfavorable for the water molecules to coexist with the polymer and undergo hydrogen bonding in the presence of higher amounts of methyl groups. Hence, a lower amount of water is absorbed at equilibrium by materials with a higher TMHDI content. With fewer water molecules between adjacent chains, i.e. lower amount of equilibrium absorption of water or swelling, the increase in polymer chain mobility is lower, leading to a lower depression in *Tg* in the 100TM composition. Conversely, a higher water absorption or swelling leads to a higher increase in mobility and hence a higher depression in *Tg* in the 0TM composition.

The primary goal of this study was to achieve improved control over the rate of actuation of SMP foam to enhance its use in a device for aneurysm treatment. The SMP foam devices are proposed to be delivered to the aneurysm site via a catheterization process while they are in their completely compressed rod-like secondary shape. As the device approaches the aneurysm site,

the clinician must carefully position the device within the aneurysm so that it does not protrude into the parent artery. Ideally, the device should not start expanding until these steps of delivery and positioning are completed. However, after these steps are complete, the device should expand at a relatively fast rate to fill the aneurysm. In this regard, a concern with moisture sensitive SMP devices is that the guiding catheters and microcatheters used in surgical processes are routinely flushed with saline solution during the device delivery. This may cause a moisture-sensitive material to potentially begin expanding inside the catheter during the delivery process. It is therefore desirable to reduce the moisture sensitivity of the device such that it is able to withstand body temperature fluid environments without actuation during the entire duration of its delivery and positioning. This duration can range from 1 minute to up to 5-10 minutes, depending on the patient vasculature and the location of the aneurysm. (Personal Communication, Dr. Hartman).

This work demonstrated that increasing the hydrophobicity of the monomers in the foam synthesis can reduce its rate of actuation. This would allow the device to initially maintain its near-compressed shape for a longer period in water/physiological environments, and later still actuate to its primary shape in a passive/active manner to fill the aneurysm. The passive actuation of a device on exposure to water/physiological media may allow the usage of a simpler deployment device without a heating capability. However, it presents a practical tradeoff in the rate of actuation vs. the working time of the device (time for which the device maintains its near-compressed secondary shape while being exposed to water/physiological media). A lower rate of actuation gives a longer device working time (as in 100TM foams, Figure 8), but complete actuation also takes a relatively long time, which may not be preferable in all cases.

A possible strategy to mitigate the tradeoff between the rate of actuation and the working time is to use a material that has high hydrophobicity to facilitate delivery and positioning of the device, and thereafter actuate it actively by applying thermal energy. The actuation temperature of these materials can be changed by varying the ratio of the hydroxyl components HPED and TEA, as reported in Singhal et al. [11], so that they may be actuated with a relatively small amount of thermal energy to minimize the potential for thermal tissue damage. Employing active actuation of the device while utilizing the above polymer synthesis toolbox is thus expected to give a higher level of predictability and control on the actuation of the SMP foam devices during their deployment for *in vivo* embolic or regenerative applications.

Conclusion

Some polyurethane SMP foams are seen to undergo premature moisture-induced actuation which may inhibit their use in transcatheter device delivery applications. To address this issue, a series of novel low density, highly covalently crosslinked SMP foams were synthesized with varying hydrophobicity by substituting HDI with a more hydrophobic TMHDI in the foam composition. Contact angle and water uptake measurements confirmed that the hydrophobicity of these materials could be controllably increased via increase in the TMHDI content, consistent with the calculated solubility parameter values. Also, the depressed *Tg* could be controlled from ~12 ºC (for 0TM foams) to ~40 ºC (for 100TM foams) after submersion in water. A reduction in the foam actuation rate corresponding to the depressed *Tg* value was observed, and time of complete actuation of a compressed foam device could be controlled from within 2 minutes (for 0TM foams) to up to more than 24 hours (for 100TM foams). Such control over the actuation rate of SMP foams by virtue of their composition has, to our knowledge, not been reported before. This

work provides the basis of a polymer synthesis toolbox that, we expect, will be useful in the development of passively or actively actuating, embolic/regenerative porous SMP scaffolds for biomedical applications.

Acknowledgement: This work was partially performed under the auspices of the U.S. Department of Energy by Lawrence Livermore National Laboratory under Contract DE-AC52-07NA27344 and supported by the National Institutes of Health/National Institute of Biomedical Imaging and Bioengineering Grant R01EB000462 and by Lawrence Livermore National Laboratory Directed Research and Development (LDRD) Grants 04-LW-054 and 04-ERD-093. The authors would like to acknowledge Thomas Yong Han (LLNL) for his help in the contact angle measurements and technical discussions.

Received: ((will be filled in by the editorial staff)); Revised: ((will be filled in by the editorial staff)); Published online: ((please add journal code and manuscript number, e.g., DOI: 10.1002/macp.201100001))

Keywords: Actuation rate, Biomaterials; Hydrophobicity; Polyurethanes; Shape memory foam

Figures and Tables

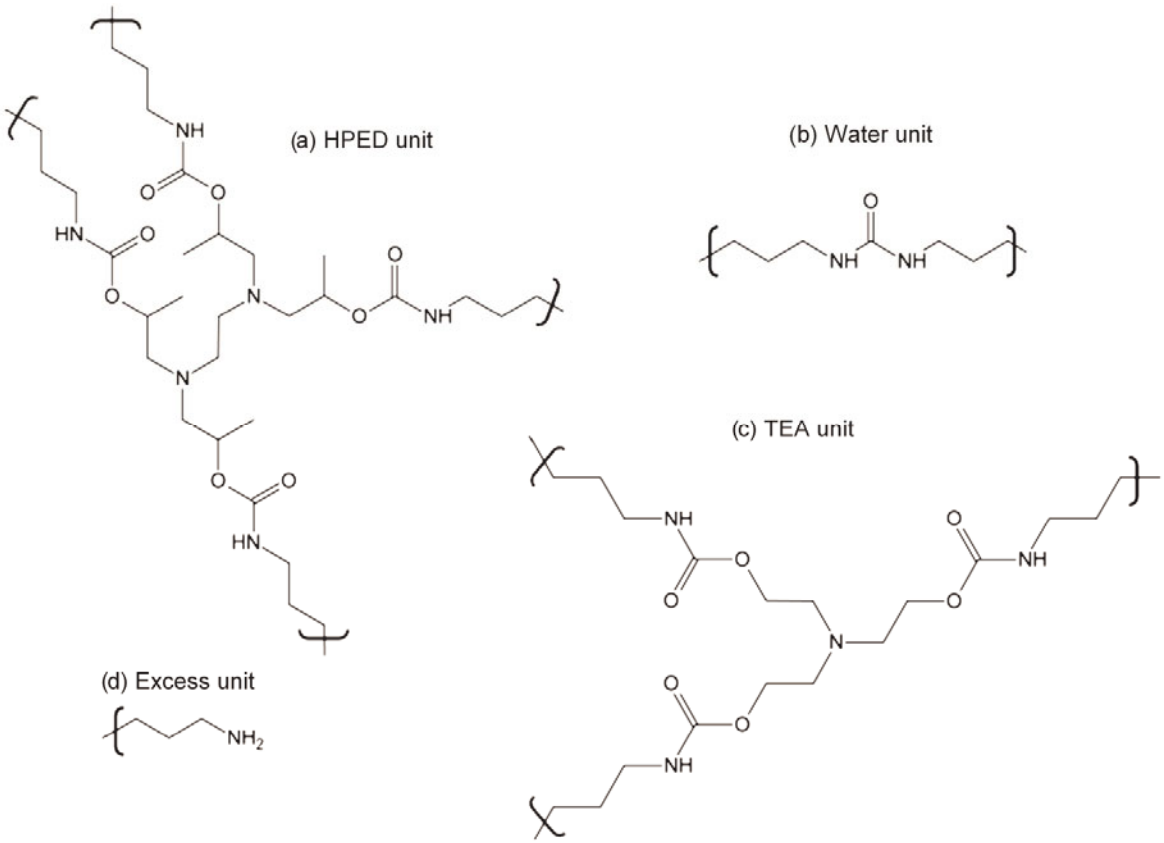

Figure 1. Structures of the (a) HPED, (b) TEA, (c) water, and (d) excess network units used to calculate the contributions of Hoy's solubility parameter components.

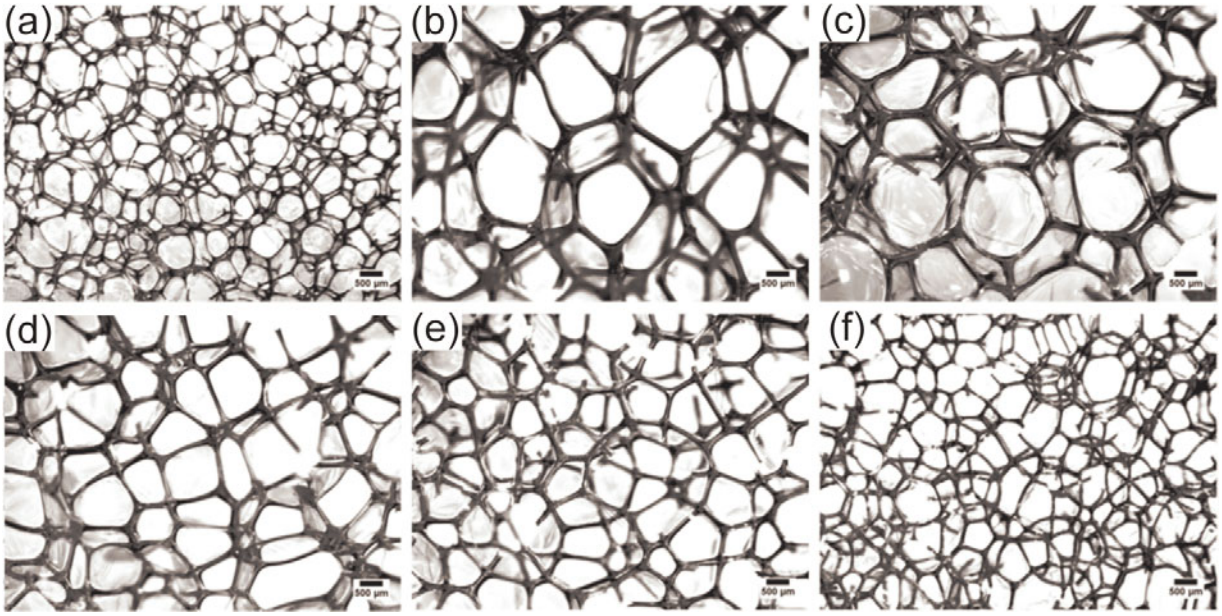

Figure 2. Cell structure of the foams as obtained from optical microscopy. Images (a), (b), (c), (d), (e) and (f) represent 0TM, 20TM, 40TM, 60 TM, 80TM and 100TM compositions, respectively (scale bar is 500 microns).

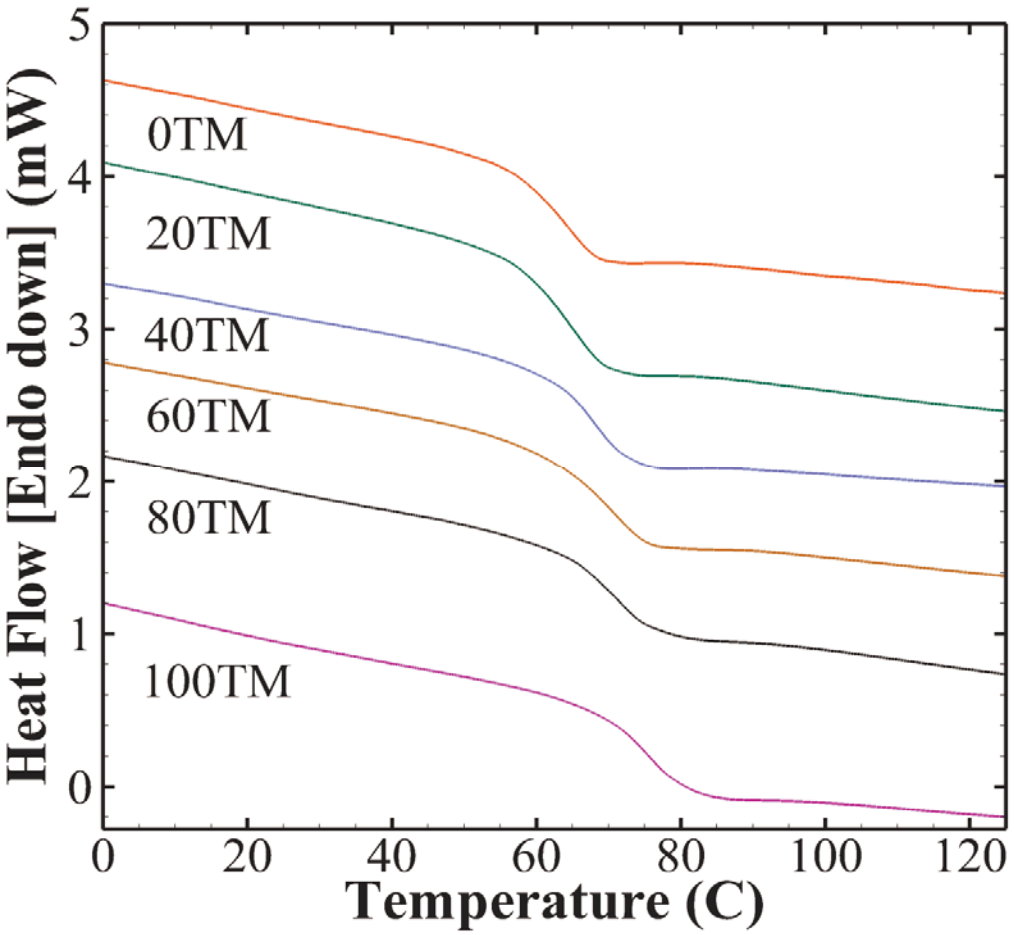

Figure 3. DSC curves of the different foam compositions. Single sharp glass transitions were seen for all compositions within a small range of 63-75 ºC.

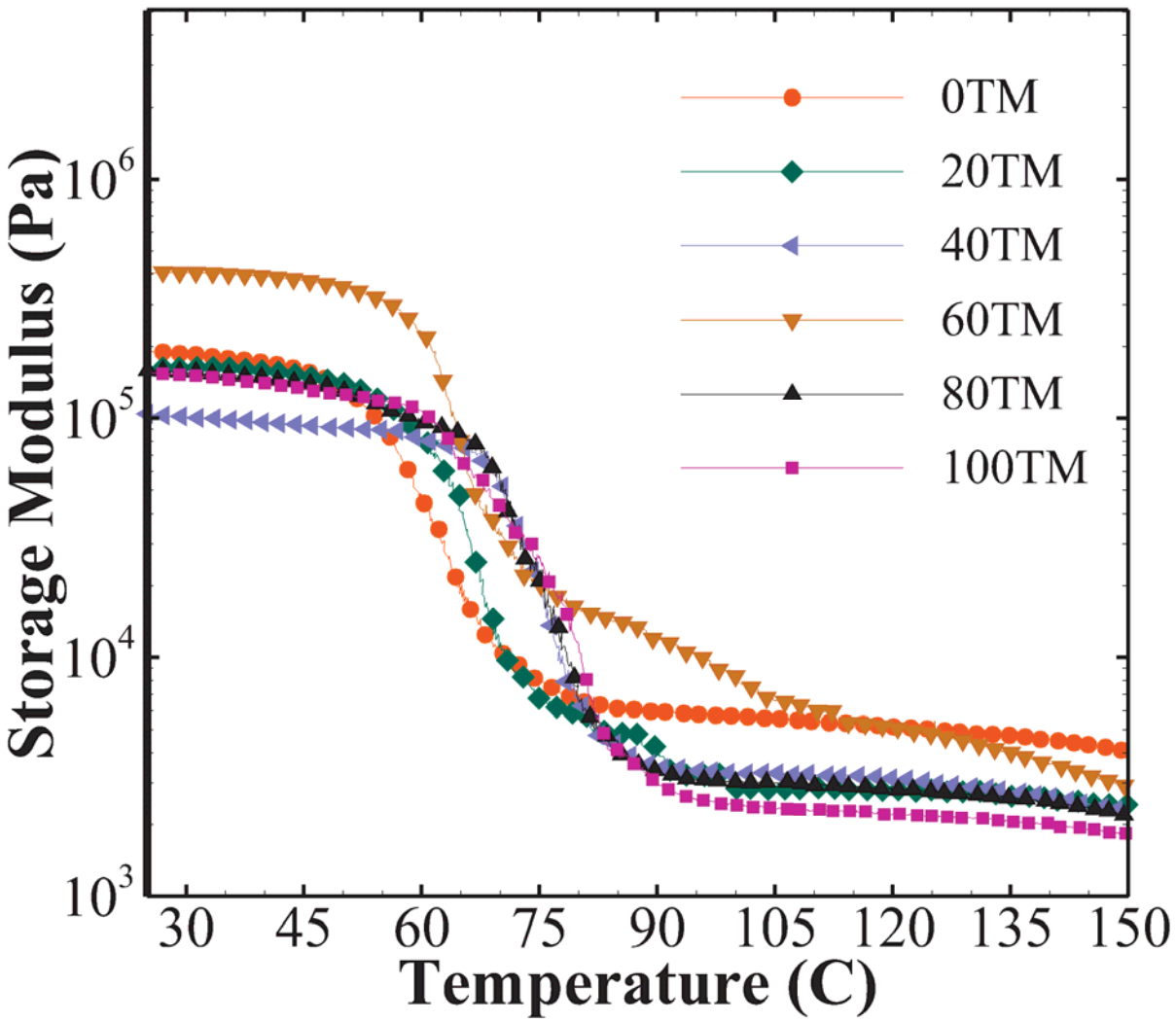

Figure 4. DMA curves of the different foam compositions. Single sharp glass transitions were seen for all compositions within a small range of 64-80 ºC.

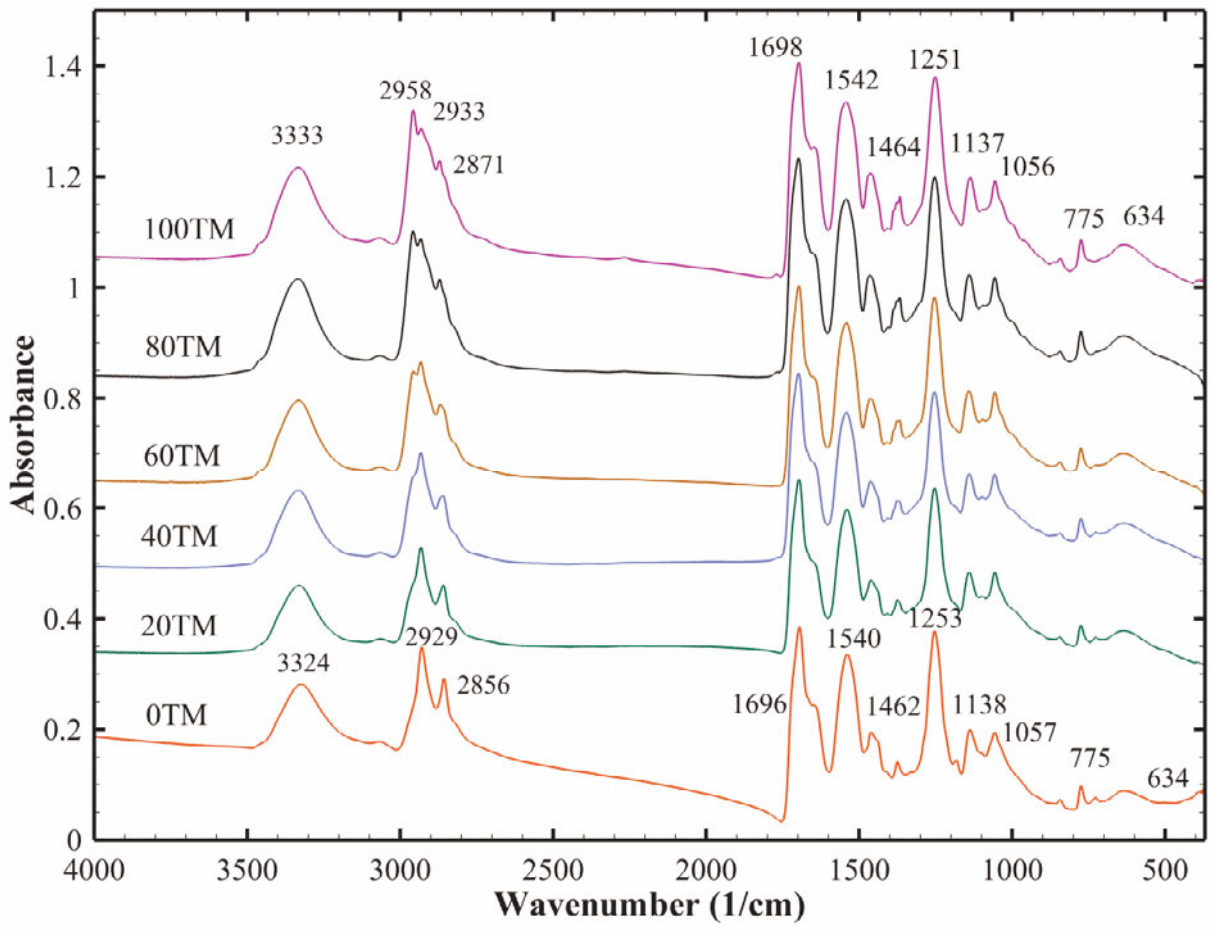

Figure 5. FTIR curves of the different foam compositions. Changes in the C-H vibrations of the -CH_3 groups of TMHDI are evident in the 2800-3000 cm^{-1}, 1430-1490 cm^{-1}, and 1350-1400 cm^{-1} ranges.

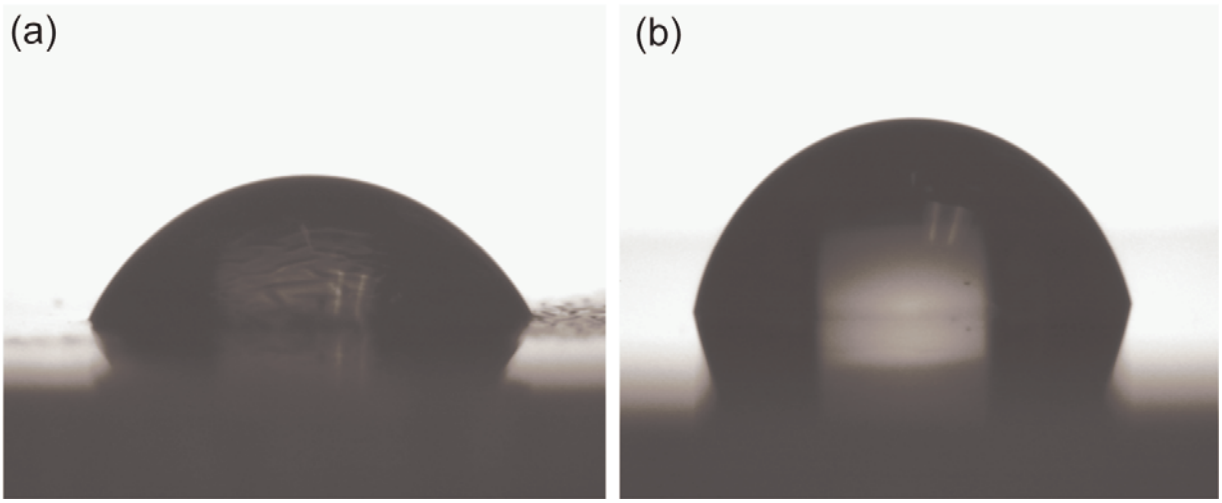

Figure 6. Contact angle images of (a) 0TM and (b) 100TM neat/unfoamed polymer compositions. An increase in the contact angle is noticed with an increase in the TMHDI content of the polymer.

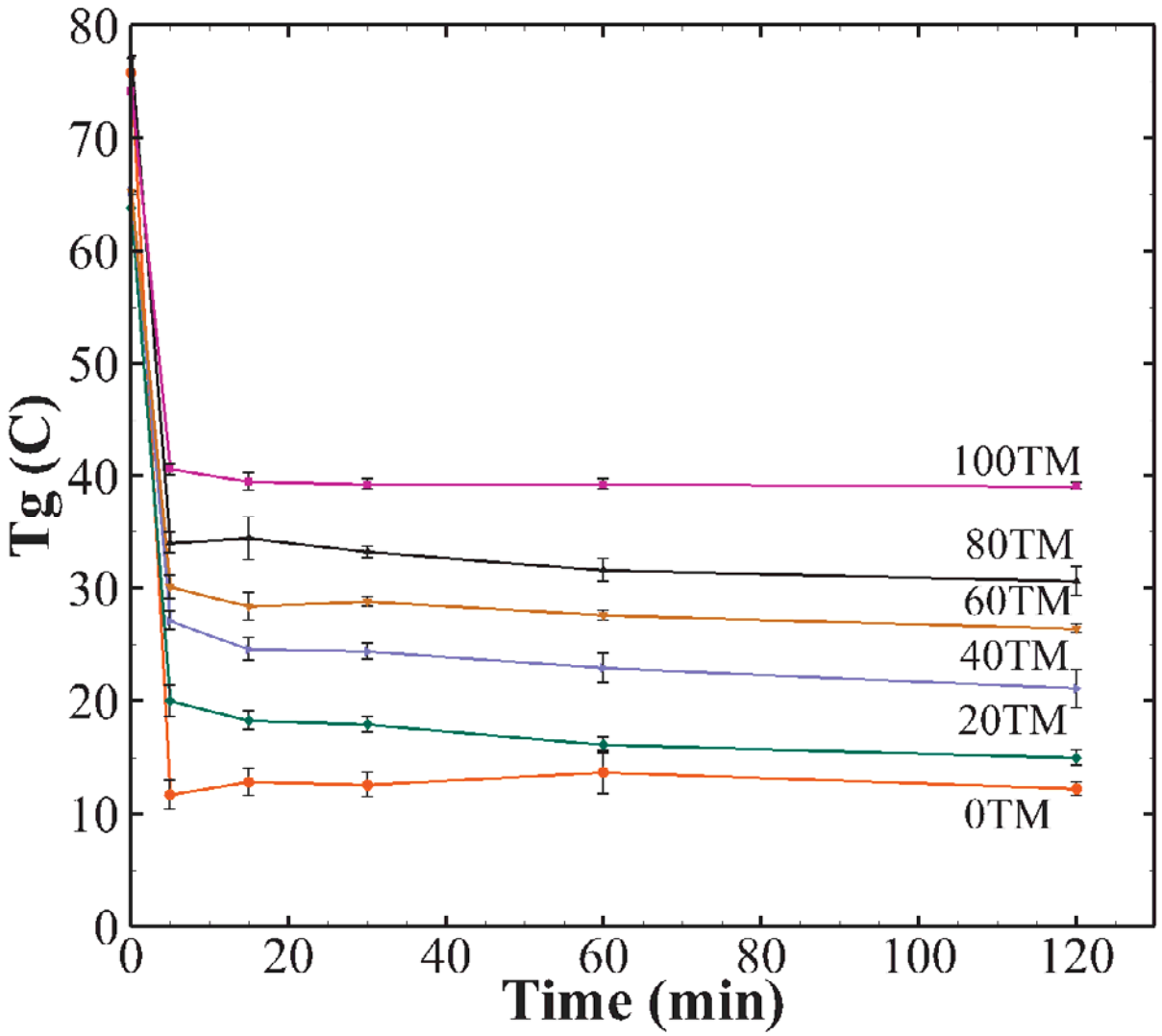

Figure 7. Change in the glass transition temperature (*Tg*) of the foam samples with respect to time submerged in water at 37 ºC. The equilibrium *Tg* value is achieved within 5 minutes for all compositions. An increase in the equilibrium *Tg* of the foams is noticed with the increase in the TMHDI content.

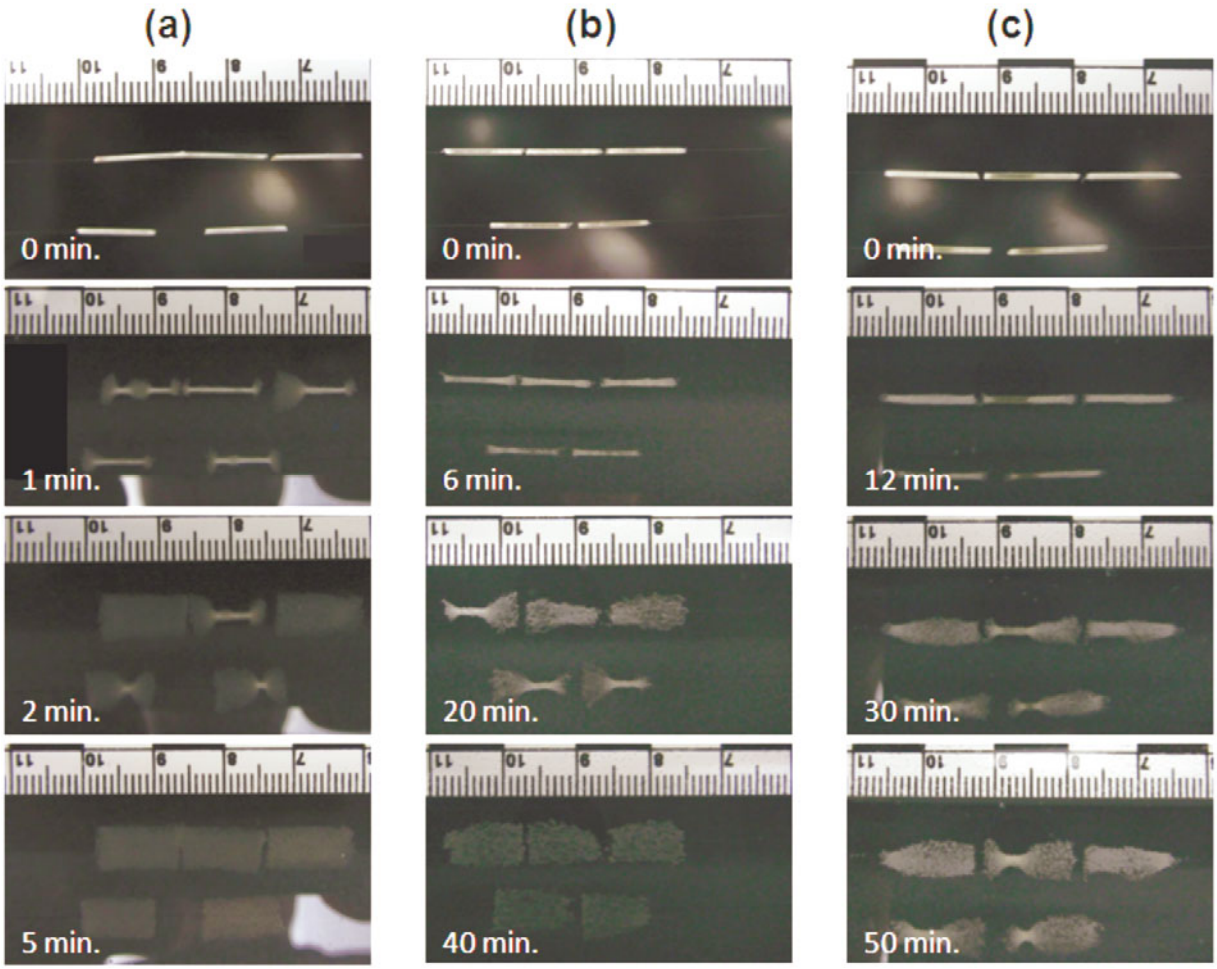

Figure 8. Rate of actuation of foam samples of (a) 0TM, (b) 80TM and (c) 100TM compositions. While the 0TM foams with only HDI in their composition actuated completely within 5 minutes of exposure to water at 37 ºC, the 100TM foams did not complete their actuation even at 50 minutes.

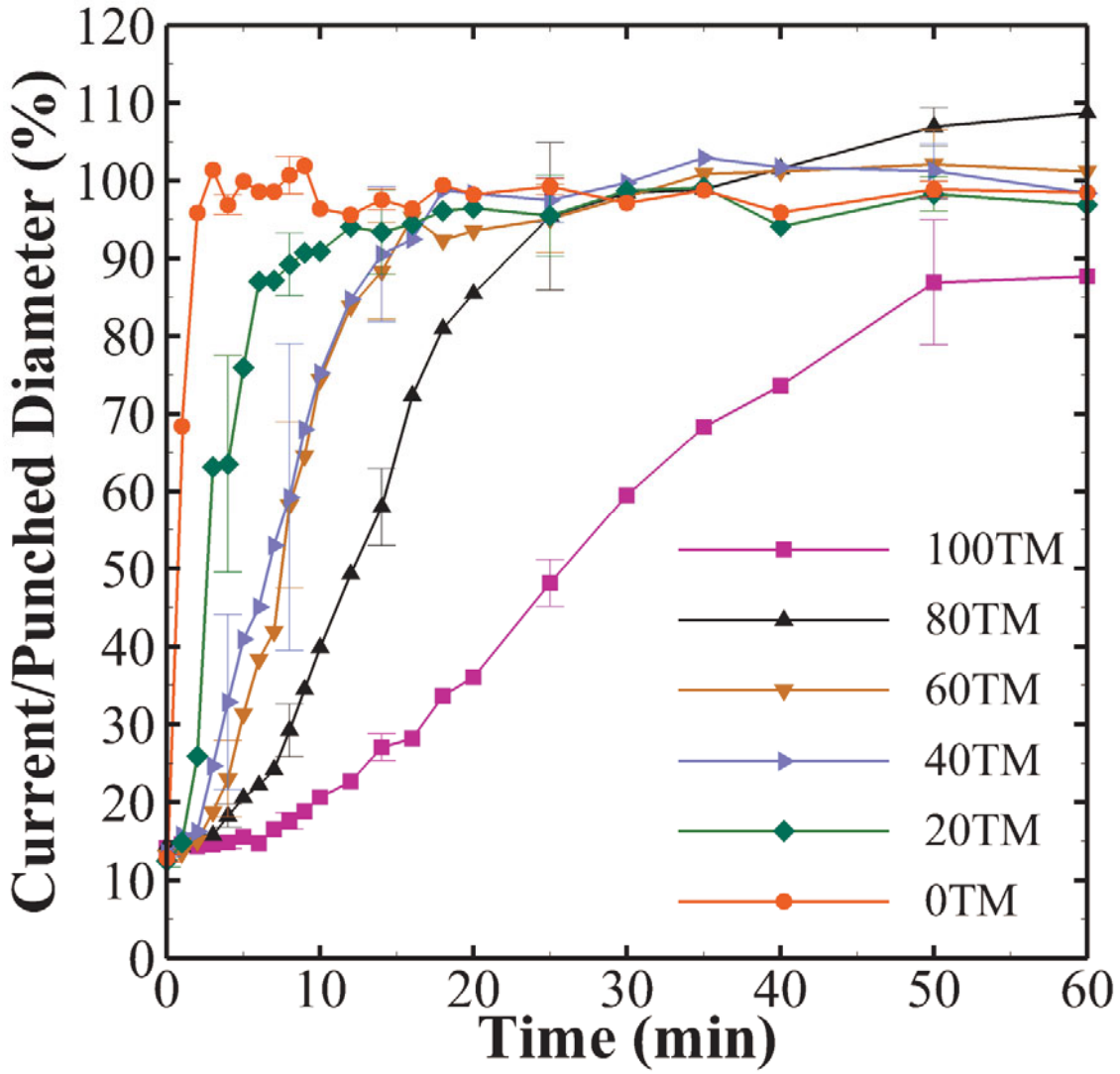

Figure 9. Ratio of the maximum diameter to the initial/punched diameter as a function of time in 37 ºC water for all foam compositions. Only every fourth error bar is marked for clarity. A decrease in the rate of expansion of the SMP foam is seen with an increase in the TMHDI content.

Table 1. Composition of foams synthesized using Hexamethylene Diisocyanate (HDI) and Trimethyl Hexamethylene Diisocyanate (TMHDI) for the isocyanate component of the urethane.

Sample ID	**HDI (wt.%)**	**TMHDI (wt.%)**	**HPED (wt.%)**	**TEA (wt.%)**	**Water (wt.%)**	**DC5179 (wt.%)**	**DCI990 (wt.%)**	**T-131 (wt.%)**	**BL-22 (wt.%)**	**Enovate (pph)**
100TM	0.00	66.79	17.11	5.73	2.35	3.81	3.30	0.26	0.64	7.62
80TM	11.00	55	17.63	5.92	2.42	3.8	3.29	0.25	0.64	7.6
60TM	22.70	42.58	18.18	6.09	2.49	3.78	3.28	0.25	0.64	7.57
40TM	35.15	29.30	18.77	6.29	2.57	3.77	3.27	0.25	0.64	7.54
20TM	48.43	15.14	19.39	6.50	2.66	3.75	3.25	0.25	0.63	7.50
0TM	62.62	0.00	20.06	6.72	2.75	3.73	3.24	0.25	0.63	7.47

Table 2. Composition of neat/non-porous polymers synthesized following the same synthesis scheme as that of the foams (Table 1). Amount of TMHDI was gradually increased from 0TM (all HDI) to 100TM (all TMHDI) composition. No foaming additives such as surfactants, catalysts and physical and chemical blowing agents were added.

Sample ID	**HDI (wt.%)**	**TMHDI (wt.%)**	**HPED (wt.%)**	**TEA (wt.%)**
100TM	0.00	61.65	28.72	9.62
80TM	10.11	50.57	29.45	9.87
60TM	20.75	38.91	30.21	10.12
40TM	31.95	26.63	31.02	10.39
20TM	43.77	13.68	31.87	10.68
0TM	56.26	0.00	32.77	10.98

Table 3. Summary of the key physical properties of the different foam compositions.

Sample ID	**Density ($g \cdot cm^{-3}$)**	***Tg*** **(°C)**	***G'*** $_{glassy}$ **at $T_{\delta s}$-20 °C (kPa)**	***G'*** $_{rubbery}$ **at $T_{\delta s}$+20 °C (kPa)**	T_{onset} **(°C)**	$T_{\delta s}$ **(°C)**	ΔT **(°C)**	***Tan δ*** **(Peak value)**
100TM	.014±.001	75	108±7	2±1	58±1	80±1	40±0	1.04±.02
80TM	.013±.002	71	103±6	3±1	57±2	77±1	42±1	1.05±.06
60TM	.025±.001	69	311±28	13±2	53±1	70±3	37±1	0.91±.01
40TM	.017±.001	68	90±3	3±2	57±3	77±1	35±3	1.02±.02
20TM	.027±.006	65	158±24	6±2	53±3	66±3	27±4	0.89±.04
0TM	0.018±.004	63	155±46	6±1	51±2	64±1	30±4	0.71±.04

Table 4. Summary of the results related to the actuation behavior of the foams.

Sample ID	**Equilibrium moisture uptake (wt.%)**	**Contact angle (Degrees)**	**Equilibrium *Tg* [1] (°C)**	**Estimated Working Time [2] (minutes)**
100TM	2.3±1.0	78.08 ± 2.58	39.1 ± 0.3	10
80TM	4.3±0.7	74.73 ± 2.51	30.6 ± 1.3	5
60TM	4.4±0.9	74.06 ± 0.83	26.4 ± 0.4	4
40TM	6.0±0.8	70.62 ± 3.51	21.1 ± 1.7	3
20TM	5.0±0.8	66.26 ± 4.97	15.0 ± 0.7	<3
0TM	8.1±1.9	62.55 ± 2.86	12.2 ± 0.6	<1

[1]Measured after 2 hours of submersion in water.

[2]Defined here as the time until ~20% of the initial diameter is recovered in 37 °C water (representative of, but not necessarily equivalent to, the working time for an actual catheter-delivered device).

Table 5. Hoy's solubility parameters calculated for the different foam compositions.

Sample ID	δ_d ($J^{1/2}\cdot cm^{-3/2}$)	δ_p ($J^{1/2}\cdot cm^{-3/2}$)	δ_h ($J^{1/2}\cdot cm^{-3/2}$)	δ_t ($J^{1/2}\cdot cm^{-3/2}$)
100TM	16.7	10.6	7.8	21.3
80TM	16.6	10.8	8.5	21.6
60TM	16.7	11.1	8.8	21.9
40TM	16.7	11.3	9.3	22.2
20TM	16.7	11.6	9.8	22.6
0TM	16.7	11.9	10.4	23.0

Table of Contents *(limit 400 characters)*

A controlled rate of actuation of ultra low density shape memory polymer (SMP) foams in water is reported. The time of complete shape recovery was controlled from within 2 minutes to up to more than 24 hours based on the material composition. This ability to control the actuation rate may significantly improve the delivery of an SMP device under conditions, such as catheterization, which require it to be exposed to high humidity/moisture environments prior to actuation.

Pooja Singhal, Anthony Boyle, Stephen Infanger, Steve Letts, Ward Small, Ya-Jen Yu, Duncan J. Maitland*, Thomas S. Wilson*

Controlling the Actuation Rate of Low Density Shape Memory Polymer Foams in Water

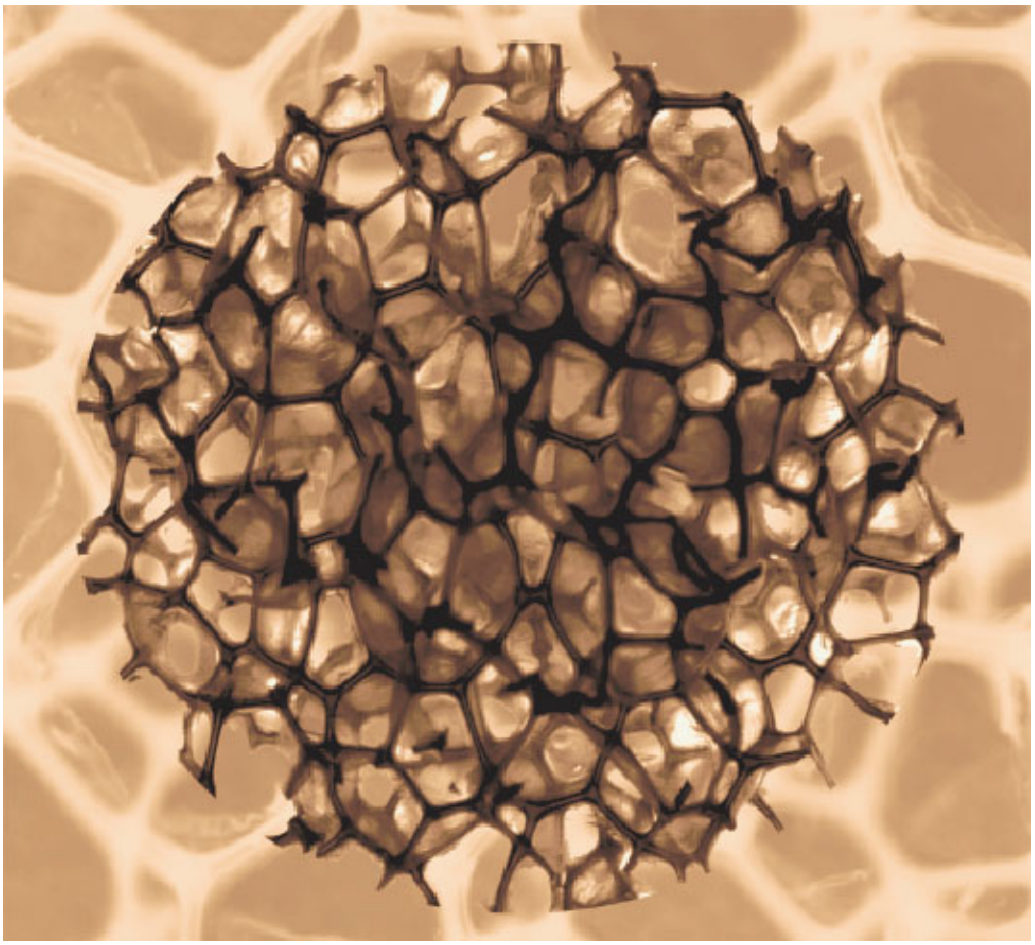

Bibliography

[1] C. Liu, H. Qin, P. T. Mather, *J. Mater. Chem.* 2007, **17**, 1543-1558.
[2] A. Lendlein, S. Kelch, *Angew. Chem. Int. Ed.* 2002, **41**, 2034-2057.
[3] P. T. Mather, X. Luo, I. A. Rousseau, *Annu. Rev. Mater. Res.* 2009, **39**, 445 - 471.
[4] I. A. Rousseau, *Polym. Eng. Sci.* 2008, **48**, 2075-2089.
[5] M. Behl, A. Lendlein, *Mater. Today.* 2007, **10**, 20 - 28.
[6] US. 5049591 (1991), Mitsubishi Jukogyo Kabushiki Kaisha, invs.: S. Hayashi, H. Fujimura.
[7] H. Tobushi, K. Okumura, M. Endo, S. Hayashi, *J. Intel. Mater. Syst. Str.* 2001, **12**, 283-287.
[8] H. Tobushi, D. Shimada, S. Hayashi, M. Endo, *Proc. Inst. Mech. Eng. L J. Mater. Des. Appl.* 2003, **217**, 135-143.
[9] H. Tobushi, R. Matsui, S. Hayashi, D. Shimada, *Smart Mater. Struct.* 2004, **13**, 881-887.
[10] L. De Nardo, R. Alberti, A. Cigada, L. H. Yahia, M. C. Tanzi, S. Farč, *Acta Biomater.* 2009, **5**, 1508-1518.
[11] P. Singhal, J. N. Rodriguez, W. Small, S. Eagleston, J. Van de Water, D. J. Maitland, T. S. Wilson, *J. Polym. Sci., Part B: Polym. Phys.* 2012, **50**, 724-737.
[12] M. A. Di Prima, M. Lesniewski, K. Gall, D. L. McDowell, T. Sanderson, D. Campbell, *Smart Mater. Struct.* 2007, **16**, 2330-2340.
[13] L. Domeier, A. Nissen, S. Goods, L. Whinnery, J. McElhanon, *J. Appl. Polym. Sci.* 2010, **115**, 3217-3229.
[14] W. M. Sokolowski, S. Hayashi. Applications of cold hibernated elastic memory (CHEM) structures. In: Proc. SPIE 10th Int. Sym. on Smart Struct. Mater., A. M. Baz, editor; 2003; San Diego (USA). p 534-544.
[15] A. Metcalfe, A. C. Desfaits, I. Salazkin, L. Yahia, W. M. Sokolowski, J. Raymond, *Biomaterials.* 2003, **24**, 491-497.
[16] W. Small, P. R. Buckley, T. S. Wilson, W. J. Benett, J. Hartman, D. Saloner, D. J. Maitland, *IEEE T. Biomed. Eng.* 2007, **54**, 1157-1160.
[17] F. El Feninat, G. Laroche, M. Fiset, D. Mantovani, *Adv. Eng. Mater.* 2002, **4**, 91-104.
[18] W. M. Sokolowski, A. Metcalfe, S. Hayashi, L. Yahia, J. Raymond, *Biomed. Mater.* 2007, **2**, S23-S27.
[19] D. J. Maitland, W. Small IV, J. M. Ortega, P. R. Buckley, J. Rodriguez, J. Hartman, T. S. Wilson, *J. Biomed. Opt.* 2007, **12**, 030504 1-3.
[20] B. Yang, W. M. Huang, C. Li, C. M. Lee, L. Li, *Smart Mater. Struct.* 2004, **13**, 191-195.
[21] Y. J. Yu, K. Hearon, T. S. Wilson, D. J. Maitland, *Smart Mater. Struct.* 2011, **20**, 085010 1-6.
[22] W. M. Huang, *The Open Medical Devices Journal.* 2010, **2**, 11-19.
[23] W. M. Huang, B. Yang, Y. Zhao, Z. Ding, *J. Mater. Chem.* 2010, **20**, 3367-3381.
[24] Y. C. Jung, H. H. So, J. W. Cho, *J. Macromol. Sci., Phys.* 2006, **45**, 453-461.
[25] B. Yang, W. M. Huang, C. Li, L. Li, *Polymer.* 2006, **47**, 1348-1356.
[26] D. Klempner, V. Sendijarevic, *Handbook of polymeric foams and foam technology*, 2nd edition. Hanser Gardner Publications, Cincinnati OH 2004.
[27] EP. 1,622,695 (2008), Porvair PLC, invs.: R. A. Olson III, P. K. Steppe.
[28] US. 2,900,278 (1959), Scott Paper Company PA, invs.: W. Powers, R. Volz.
[29] US. 3,171,820 (1965), Scott Paper Company PA, invs.: R. Volz.
[30] US. 3,125,542 (1964), Owens-Corning Fiberglas Corp DE, invs.: R. M. Haines.
[31] US. 3,175,030 (1965), Chemotronics Inc. MI, invs.: H. Geen.
[32] US. 3,175,025 (1965), Chemotronics Inc. MI, invs.: H. Geen, W. Rice.
[33] US. 2,961,710 (1960), Norman H. Stark, invs.: N. H. Stark.
[34] J. S. Mijovik, J. A. Koutsky, *Polym. Plast. Technol. Eng.* 1977, **9**, 139-179.

[35] C. M. Yakacki, R. Shandas, D. Safranski, A. M. Ortega, K. Sassaman, K. Gall, *Adv. Func. Mater.* 2008, **18**, 2428-2435.
[36] D. W. Van Krevelen, K. Te Nijenhuis, *Properties of polymers: their correlation with chemical structure, their numerical estimation and prediction from additive group contributions*, 4th edition. Elsevier, Amsterdam 2009.
[37] L. J. Gibson, M. F. Ashby, G. S. Schajer, C. I. Robertson, *Proc. R. Soc. A.* 1982, **382**, 25-42.
[38] P. R. Onck, E. W. Andrews, L. J. Gibson, *Int. J. Mech. Sci.* 2001, **43**, 681-699.
[39] E. W. Andrews, G. Gioux, P. Onck, L. J. Gibson, *Int. J. Mech. Sci.* 2001, **43**, 701-713.
[40] D. Welti, *Infrared Vapour Spectra: Group Frequency Correlations, Sample Handling and the Examination of Gas Chromatographic Fractions*, illustrated edition, Heyden & Sons, London 1970.
[41] G. Socrates, *Infrared Characteristic Group Frequencies: Tables and Charts*, 2nd edition. Wiley & Sons, New York 1994.
[42] R. M. Hodge, T. J. Bastow, G. H. Edward, G. P. Simon, A. J. Hill, *Macromolecules.* 1996, **29**, 8137-8143.